Stress dependence of the hysteresis loops of Co-rich amorphous wire

1998 J. Phys.: Condens. Matter 10 2453

(http://iopscience.iop.org/0953-8984/10/11/009)

J. Phys.: Condens. Matter **10** (1998) 2453–2463. Printed in the UK PII: S0953-8984(98)79852-2

Stress dependence of the hysteresis loops of Co-rich amorphous wire

N Usov†, A Antonov‡, A Dykhne† and A Lagar'kov‡

† Troitsk Institute for Innovation and Fusion Research, 142092, Troitsk, Moscow Region, Russia
‡ Scientific Centre for Applied Problems in Electrodynamics, Moscow, Russia

Received 26 November 1996, in final form 25 September 1997

Abstract. The structure of the 90° domain wall separating the inner core and the outer shell of Co-rich amorphous wire is studied theoretically on the basis of a model distribution of the residual quenching stresses throughout the wire volume. For a long wire, both axial and circumferential hysteresis loops are obtained at different values of the applied stress. The applied tensile stress is shown to reduce the remanent wire magnetization, but has only little effect on the wire coercivity. On the other hand, the applied torsional stress leads to an increase of the wire coercivity. The results obtained are in qualitative agreement with recent experiments.

1. Introduction

The properties of soft ferromagnetic wires produced by the 'in-rotating-water' quenching technique attract considerable research interest due to some unique characteristics, such as magnetic bistability, mainly observed in Fe-rich materials, and the Matteuci effect (see reviews [1–3] and references therein). More recently [4–5], the giant magneto-impedance (GMI) effect has been reported for Co-rich amorphous wires and ribbons with very small magnetostriction constants. The great sensitivity of the effect to the external magnetic field makes it very promising for applications in new magnetic sensors and magnetic recording heads.

To understand the origin of the GMI effect it seems important to study the influence of external magnetic field on a very sensitive magnetization distribution in Co-rich amorphous wire with nearly zero magnetostriction. The magnetic properties of amorphous wires are usually explained in terms of the so-called core–shell domain structure [1–3, 6]. In the case of Co-rich amorphous wire with negative magnetostriction, the model consists of the inner core uniformly magnetized along the wire axis and the outer shell with circumferential magnetization. It is supposed that the distribution of the residual quenching stresses throughout the wire volume plays a decisive role in determining its magnetization configuration. In this paper we study theoretically what kind of residual stress distribution results in the core–shell domain structure in Co-rich amorphous wire. We analysed also the effect of the external magnetic field as well as the influence of applied stresses on the magnetization distribution in Co-rich amorphous wire. The results obtained are compared with the relevant experimental data.

0953-8984/98/112453+11$19.50

2. The structure of the 90° domain wall

It is generally accepted [1–3] that owing to the lack of magnetocrystalline anisotropy the magnetic anisotropy of amorphous wires is mainly determined by magnetoelastic interactions. The latter originate in amorphous wires due to residual quenching stresses. In accordance with this idea, here we postulate that the magnetoelastic energy density of an amorphous wire is given by [7]

$$w_{m-el}^{(1)} = -\frac{3}{2}\lambda_s(\sigma_{\rho\rho}^{(q)}\alpha_\rho^2 + \sigma_{\varphi\varphi}^{(q)}\alpha_\varphi^2 + \sigma_{zz}^{(q)}\alpha_z^2) \tag{1}$$

where λ_s is the saturation magnetostriction constant, $\sigma_{ii}^{(q)}$ are the diagonal components of the residual stress tensor in cylindrical coordinates (ρ, φ, z) and α_i are the components of the unit magnetization vector. The nondiagonal components of the stress tensor are assumed to vanish due to the symmetry of the in-rotating-water quenching procedure. For the same reason the values $\sigma_{ii}^{(q)}$ are assumed to be functions of the reduced variable $x = \rho/R$ only, R being the wire radius.

Let us prove that equation (1) determines the easy-axis distribution throughout the wire volume. In fact, it is a quadratic form with respect to the components of the unit magnetization vector. It is easy to see that in the case of Co-rich amorphous wire with $\lambda_s < 0$, the quadratic form (1) has a minimum when the unit magnetization vector points along the direction corresponding to the smallest of the components $\sigma_{ii}^{(q)}$. Therefore, the direction of the easy axis in the amorphous wire with the magnetoelastic energy density given by equation (1) is determined by the relative values of the functions $\sigma_{ii}^{(q)}(x)$ with respect to each other.

Though some attempts have been made [8, 9] to calculate the residual stress tensor components in an amorphous wire, these calculations seem to be oversimplified, as is discussed in section 4. Furthermore, they lead to the conclusion [3] that the $\sigma_{\rho\rho}^{(q)}$-component is the smallest component near the centre of an amorphous wire. Thus, in accordance with these calculations, the easy anisotropy axis must be directed radially in the inner core region of the amorphous wire. This result seems incompatible with the conventional core–shell domain structure of Co-rich amorphous wire [1–3, 6].

In order to investigate qualitatively the role of the residual quenching stresses and to describe the experimental data properly, in this paper we use the assumption [10] that the behaviour of the diagonal components of the residual stress tensor in the amorphous wire is similar to that for the quenched materials in the form of a large rod. As the experiment [11] shows, in an iron rod the values $\sigma_{ii}^{(q)}$ are decreasing functions of x, the $\sigma_{\rho\rho}^{(q)}$-component being positive. Also, the $\sigma_{\varphi\varphi}^{(q)}$- and $\sigma_{zz}^{(q)}$-components are positive near the centre of the wire but change sign somewhere in the rod interior and become negative near the rod surface. We assume a similar dependence for the $\sigma_{ii}^{(q)}$-values for the amorphous wire, as shown schematically in the figure 1. Additionally, we try to find the simplest possible scenario leading to the core–shell magnetization distribution in the amorphous wire with negative magnetostriction.

First, consider the case shown in figure 1(a), where the inequality $\sigma_{\varphi\varphi}^{(q)} < \sigma_{\rho\rho}^{(q)}, \sigma_{zz}^{(q)}$ holds over the whole range of radii, $0 < \rho < R$, and hence the easy anisotropy axis points in the azimuthal direction everywhere. It can be shown that in this case the lowest-energy state of the wire is the magnetization curling with $\alpha_\varphi = +1$ or $\alpha_\varphi = -1$ throughout the wire volume, the uniformly magnetized core being absent. More strictly, the α_z-component remains nonzero only in the very small region $\rho < \delta$ near the wire centre, where $\delta = \sqrt{C/K_e}$ is a length of the order of the domain wall width, C is the exchange constant

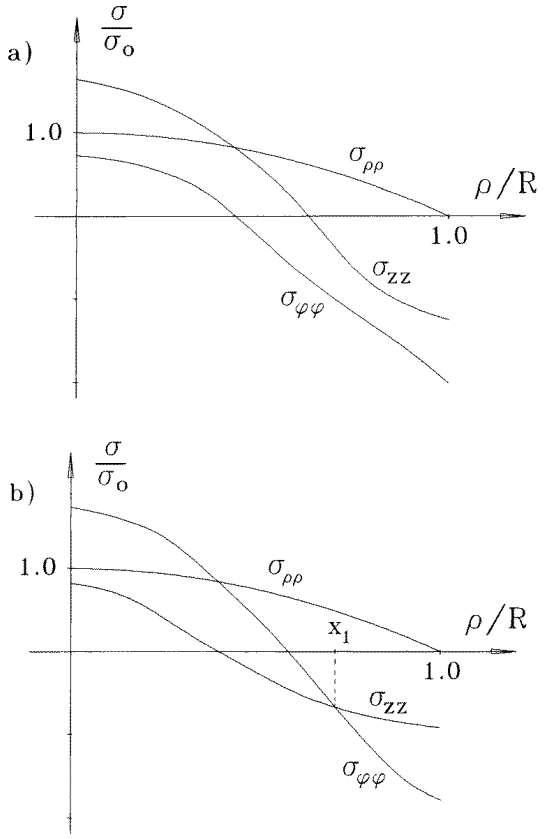

Figure 1. The assumed radial dependence of the residual stress tensor components in Co-based wire: (a) the uniformly magnetized inner core is absent; (b) the reduced inner-core radius is given by $x_1 = R_1/R$.

and K_e is the effective anisotropy constant. This excludes the magnetization singularity at $\rho = 0$ (see also [12]), but makes a very small contribution to the longitudinal wire magnetization. Thus, the situation shown in figure 1(a) is unexpected for the Co-rich Unitika wires, for which the hysteresis loop measurements show an appreciable remanent magnetization directed along the wire axis [6, 10, 13]. One can explain this fact [6] assuming that near the centre of the wire the easy anisotropy axis points in the z-direction. From equation (1) this implies that near the centre of the wire the inequality $\sigma_{zz}^{(q)} < \sigma_{\rho\rho}^{(q)}, \sigma_{\varphi\varphi}^{(q)}$ must hold, whereas the previous one holds near the wire surface (see figure 1(b)). In such a case the function $\sigma_{zz}^{(q)}(x)$ intersects $\sigma_{\varphi\varphi}^{(q)}(x)$ at a certain point $x_1 = R_1/R < 1$. It can be shown [14] that R_1 is the radius of an inner core region uniformly magnetized along the wire axis; for $\rho > R_1$ the magnetization is directed circumferentially. Of course, the wire magnetization does not change abruptly in the wire volume. Therefore, the 90° domain wall separating the core and the outer shell of the amorphous wire originates near $\rho = R_1$.

Recently, the influence of various kinds of applied stress on the magnetization distribution in an amorphous wire has been studied experimentally [13, 15, 16]. It can be theoretically described by adding some terms to the magnetoelastic energy of the wire. For example, due to the application of a uniform tensile stress to the ends of the amorphous

wire, a magnetoelastic energy density appears [7]:

$$w_{m-el}^{(2)} = -\frac{3}{2}\lambda_s \sigma_{zz}^{(a)} \alpha_z^2 \tag{2}$$

where the only nonvanishing stress tensor component is given by $\sigma_{zz}^{(a)} = \text{constant}$ [17]. On the other hand, the influence of the applied torsional stress on the wire magnetization can be described by means of the equation

$$w_{m-el}^{(3)} = -3\lambda_s \sigma_{\varphi z}^{(a)} \alpha_\varphi \alpha_z \qquad \sigma_{\varphi z}^{(a)} = \frac{E\varepsilon}{2(1+\nu)}\rho \tag{3}$$

since in this case only the component $\sigma_{\varphi z}^{(a)}$ is nonzero [17]. Here E is Young's modulus, ν is Poisson's modulus and ε is the torsional angle per unit wire length.

In this paper we confine ourselves to the case in which the magnetic anisotropy of the amorphous wire can be described by means of equations (1)–(3). We assume that the eigenstresses produced by the magnetostrictive strains of the domain walls are small in comparison with the quenching stresses due to the very low value of the saturation magnetostriction constant of Co-rich wire. One may assume that the various types of heat treatment [18] modify the as-cast stress distribution in Co-rich wire considerably. The effect of the heat treatment as well as that of the induced anisotropy can probably be taken into account qualitatively by means of the corresponding change of the stress tensor components in equation (1).

To obtain the total free energy of the amorphous wire it is necessary to take into account in addition to (1)–(3) the exchange and the Zeeman energies. We assume that the exchange energy density in amorphous wire is given by a simple equation [7]:

$$w_{exc} = \frac{C}{2}(\nabla \boldsymbol{\alpha})^2. \tag{4}$$

It should be noted that previous work on the magnetization structure of amorphous wires [6, 9, 10] has neglected the exchange energy term, taking into consideration just the distribution of the easy anisotropy energies throughout the wire cross-section. Nevertheless, it seems of interest to study the structure of a 90° domain wall separating the core and shell regions of a Co-rich wire. As we shall see below, it has a rather large width and its structure depends substantially on the values of the applied stresses.

As for the Zeeman energy, we consider two different cases. When an external magnetic field with an amplitude H_0 is applied along the wire axis, the Zeeman energy density is given by

$$w_Z^{(1)} = -M_s H_0 \alpha_z. \tag{5a}$$

On the other hand, the energy density related to a current I flowing through the wire can be evaluated as

$$w_Z^{(2)} = -M_s H_\varphi \alpha_\varphi \qquad H_\varphi = \frac{2I}{cR^2}\rho. \tag{5b}$$

In this paper we do not take end effects into consideration [19], assuming the wire to be sufficiently long for this to be appropriate. Then, bearing in mind the axial symmetry of the wire and the residual and applied stresses, one can suppose that the magnetization distribution in the wire may be expressed as

$$\alpha_\rho = 0 \qquad \alpha_\varphi = \sin\theta(\rho) \qquad \alpha_z = \cos\theta(\rho) \tag{6}$$

where $\theta(\rho)$ is a function to be determined. Note that for the magnetization distribution (6) the densities of the volume and surface magnetic charges vanish simultaneously. Thus, the magnetostatic wire energy is zero.

First, let us consider the case in which the uniform external magnetic field is applied along the wire axis. Then, the total energy of the wire with applied stresses can be obtained by means of the integration of the sum of equations (1)–(4) and (5*a*) throughout the wire volume. Taking into account (6), one can obtain

$$W = W_{exc} + W_{m-el} + W_Z^{(1)}$$

$$W_{exc} = 2\pi L_z \int_0^R \rho \, \mathrm{d}\rho \, \frac{C}{2}\left[\left(\frac{\mathrm{d}\theta}{\mathrm{d}\rho}\right)^2 + \frac{\sin^2\theta}{\rho^2}\right] \tag{7a}$$

$$W_{m-el} = \pi L_z \frac{K_e}{\sigma_0}\int_0^R \rho \, \mathrm{d}\rho \, \left[\sigma_{\varphi\varphi}^{(q)}\sin^2\theta + (\sigma_{zz}^{(q)} + \sigma_{zz}^{(a)})\cos^2\theta + 2\sigma_{\varphi z}^{(a)}\sin\theta\cos\theta\right] \tag{7b}$$

$$W_Z^{(1)} = -2\pi L_z M_s H_0 \int_0^R \rho \, \mathrm{d}\rho \, \cos\theta(\rho) \tag{7c}$$

where $K_e = 3|\lambda_s|\sigma_0$ is the effective anisotropy constant, σ_0 is the amplitude of the residual stress and L_z is the length of the wire.

Minimizing the total wire energy (7) with respect to the function $\theta(\rho)$ one arrives at the equation

$$-\frac{1}{x}\frac{\mathrm{d}}{\mathrm{d}x}\left(x\,\frac{\mathrm{d}\theta}{\mathrm{d}x}\right) + \left[\frac{1}{x^2} + p\frac{\sigma_{\varphi\varphi}^{(q)} - (\sigma_{zz}^{(q)} + \sigma_{zz}^{(a)})}{\sigma_0}\right]\sin\theta\cos\theta + p\frac{\sigma_{\varphi z}^{(a)}}{\sigma_0}\cos 2\theta + h_0\sin\theta = 0 \tag{8a}$$

with the boundary condition $\mathrm{d}\theta/\mathrm{d}x = 0$ at $x = 1$. Here we introduce the dimensionless parameters

$$p = \frac{K_e R^2}{C} \qquad h_0 = \frac{H_0 M_s R^2}{C}. \tag{8b}$$

The solution for (8) must remain finite at $x = 0$. It describes the structure of the 90° domain wall separating the inner core and the outer shell of the Co-rich wire. Simple estimations for a position and a width of the wall in the absence of applied stress were given recently [14]. Here we study the influence of the applied stresses on the wall structure.

The calculations for the case (5*b*), in which the wire magnetization is affected by the direct current I flowing through the wire, lead to the same equation (8), with the difference that the last term in this equation is replaced by the term

$$-h_\varphi x\cos\theta$$

where

$$h_\varphi = \frac{H_\varphi M_s R^2}{C}.$$

Using in (8*b*) the values $K_e = (2\text{–}4)\times 10^2$ erg cm^{-3}, $R = 6\times 10^{-3}$ cm and $C = 10^{-6}$ erg cm^{-1} [6], one can see that the parameter $p \approx 10^3$ is very large for a typical Co-rich wire. For this reason, the Runge–Kutta method usually used for numerical integration of ordinary differential equations turns out to be unsuccessful in our case. To solve this problem we use here a numerical procedure which is analogous to a direct numerical integration of the Landau–Lifshitz–Gilbert (LLG) equation [20]. The details of the calculations are given in the appendix.

The results of the calculations are shown in figures 2–4. For definiteness, we assume in these calculations that for as-cast wire the residual stress tensor components are described by means of the simple model expressions

$$\sigma_{\rho\rho}^{(q)} = \sigma_0(1-x^2) \qquad \sigma_{\varphi\varphi}^{(q)} = \sigma_0(1-2x^2) \qquad \sigma_{zz}^{(q)} = \sigma_0(0.5-x^2). \tag{9}$$

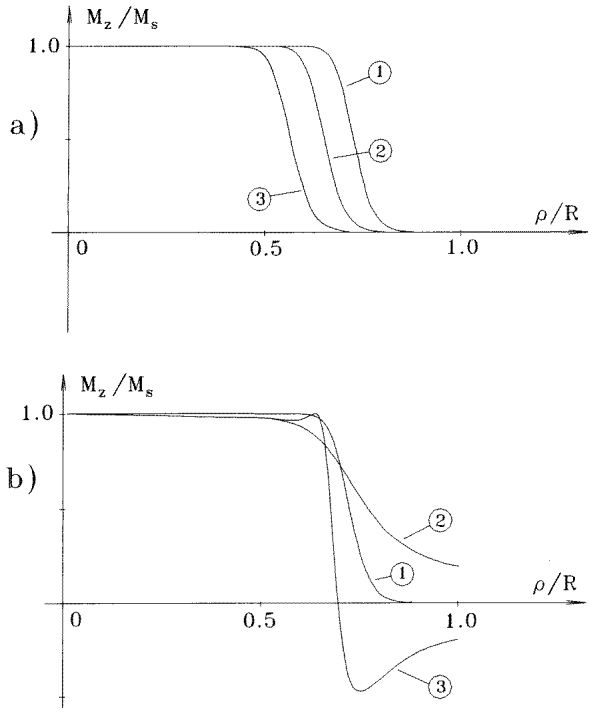

Figure 2. The structure of the 90° domain wall in amorphous Co-based wire with the radius $R = 6 \times 10^{-3}$ cm and effective anisotropy constant $K_e = 250$ erg cm^{-3} at various values of applied stress. (a) Tensile stress: (1) $\sigma_{zz}^{(a)}/\sigma_0 = 0$; (2) $\sigma_{zz}^{(a)}/\sigma_0 = 0.1$; (3) $\sigma_{zz}^{(a)}/\sigma_0 = 0.2$. (b) Torsional stress: (1) $\sigma_{\varphi z}^{\max}/\sigma_0 = 0$; (2) $\sigma_{\varphi z}^{\max}/\sigma_0 = 0.1$; (3) $\sigma_{\varphi z}^{\max}/\sigma_0 = -0.1$. $\sigma_{zz}^{(a)}/\sigma_0 = 0.2$ is the amplitude of the residual quenching stress; $\sigma_{\varphi z}^{\max}$ is the maximal value of the torsional stress at the wire surface.

Also, the effective anisotropy constant and the saturation magnetization of amorphous Co-rich wire are assumed to be $K_e = 250$ erg cm^{-3} and $M_s = 500$ G, respectively. Choosing the model expressions (9), one must take into account the condition $\langle \sigma_{zz} \rangle = 0$. In fact, one can assume that a sufficiently long piece of an amorphous wire is uniform along its length. In such a case, the above condition is a consequence of the mechanical equilibrium equation for the amorphous wire [17].

Qualitatively, the radial dependencies of the values (9) correspond to the case shown in figure 1(b). The reduced inner-core radius is the important parameter, which can be estimated for a given wire from the experiment. It is approximately determined by the relation $\sigma_{\varphi\varphi}^{(q)}(x_1) = \sigma_{zz}^{(q)}(x_1)$ [14]. Thus, for the model (9) we have $x_1 = 1/\sqrt{2}$, while the reduced remanent magnetization is $M_r/M_s \approx x_1^2 = 1/2$. We choose this value as an average one, bearing in mind that for different Co-rich wires the experimental data for the remanent ratio are scattered in the range from $M_r/M_s = 0.25$ [10] to $M_r/M_s = 0.65$ [6].

Figure 2(a) shows the influence of the applied tensile stress on the structure of the 90° domain wall in the absence of the external magnetic field. It can be seen that due to a small value of the effective anisotropy constant the width of the wall is rather large (of the order of several micrometres). Also, as a result of the tensile stress the inner-core radius of the wire reduces. In our model this can be explained as follows. From equation (8) one can see that the application of the tensile stress leads to an increase of the total longitudinal stress

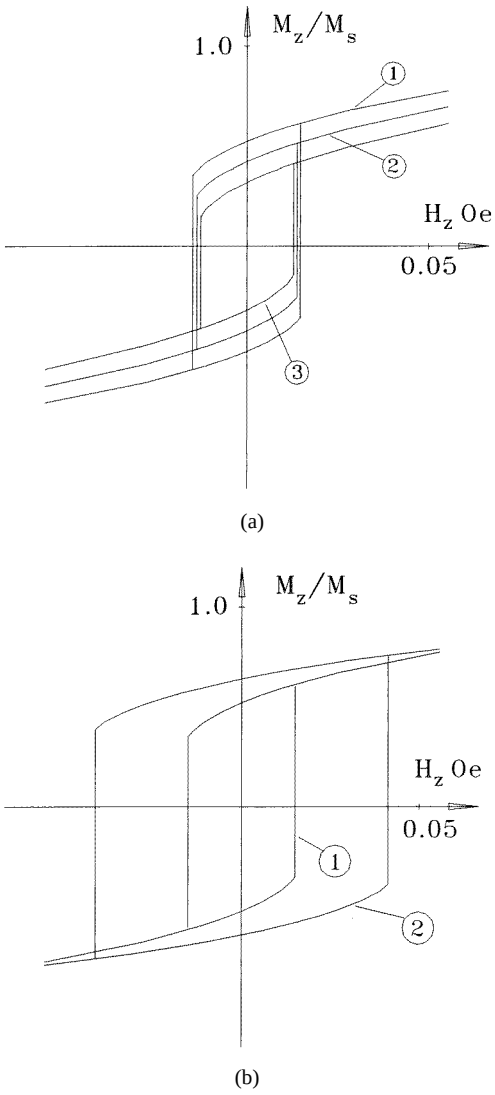

Figure 3. (a) Axial hysteresis loops of Co-rich amorphous wire at various values of applied tensile stress: (1) $\sigma_{zz}^{(a)}/\sigma_0 = 0$; (2) $\sigma_{zz}^{(a)}/\sigma_0 = 0.1$; (3) $\sigma_{zz}^{(a)}/\sigma_0 = 0.2$. (b) Axial hysteresis loops of Co-rich amorphous wire at various values of applied torsional stress: (1) $\sigma_{\varphi z}^{\max}/\sigma_0 = 0$; (2) $\sigma_{\varphi z}^{\max}/\sigma_0 = 0.1$.

tensor component. Thus, the curve corresponding to the $\sigma_{zz}^{(q)}$-component in figure 1(b) has a parallel shift upwards with respect to the curve corresponding to the $\sigma_{\varphi\varphi}^{(q)}$-component. Then, the intersection point of the curves is moved to the left and the inner-core radius reduces since the direction of the easy anisotropy axis is determined by the relative values of the $\sigma_{zz}^{(q)}$- and $\sigma_{\varphi\varphi}^{(q)}$-components.

Figure 2(b) shows the influence of the applied torsional stress on the wall structure. Here $\sigma_{\varphi z}^{\max} = E\varepsilon R/2(1+\nu)$ is the maximal value of the torsional stress at the wire surface. One can see that the magnetization distribution in the wire depends on the sign of the torsional angle ε with respect to that of the α_φ-component of the unit magnetization vector

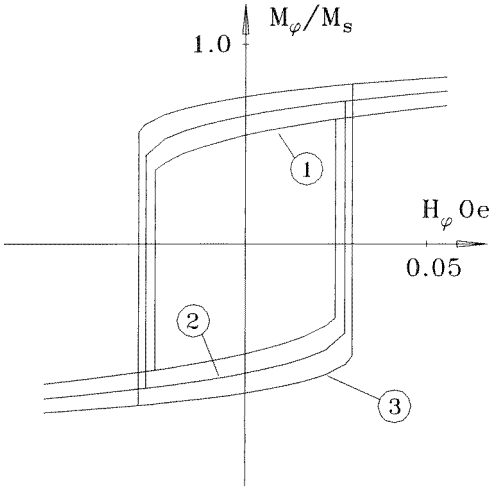

Figure 4. Circumferential dc hysteresis loops of Co-rich amorphous wire at various values of applied tensile stress: (1) $\sigma_{zz}^{(a)}/\sigma_0 = 0$; (2) $\sigma_{zz}^{(a)}/\sigma_0 = 0.1$; (3) $\sigma_{zz}^{(a)}/\sigma_0 = 0.2$. H_φ is the amplitude of the circular magnetic field at the wire surface.

in the outer shell of the wire. Curves 2 and 3 in figure 2(b) correspond to the positive and the negative values of the torsional angle, respectively. Thus, as a result of the torsional stress the magnetization distribution in the outer shell of the wire looks like a helix. The direction of the helix depends on the sign and the value of the torsional angle per unit wire length.

It should be noted that various radial dependencies of the stress tensor components similar to that of equation (9) lead to close radial magnetization profiles. Thus, we believe that the results obtained in this paper hold qualitatively for a broad enough class of expressions (9) compatible with the conventional core–shell domain structure of Co-rich amorphous wire.

3. Wire hysteresis loops

Calculating the different components of the wire magnetization at every given amplitude of the external magnetic field (or current flowing through the wire), one can obtain the various types of hysteresis loop of the amorphous Co-rich wire as shown in figures 3 and 4. Figures 3(a) and 3(b) show the axial hysteresis loops of the wire at different values of applied tensile or torsional stresses, respectively. It can be seen that the tensile stress reduces the remanent wire magnetization but does not have much effect on the wire coercivity. The reduction of the remanent magnetization may be easily explained if one takes into account that the applied tensile stress reduces the inner-core radius of the wire (see figure 2(a)). On the other hand, the applied torsional stress of positive sign leads to an increase in the average longitudinal wire magnetization (see curve 2 in figure 2(b)). As a result, the remanent wire magnetization also increases. It should be mentioned that the shape of the hysteresis loop depends on the relative signs of the tensor component $\sigma_{\varphi z}^{(a)}$ and the α_φ-component of the unit magnetization vector in the outer shell of the wire. Curve 2 of figure 3(b) is the limited loop corresponding to the case in which the signs of the two components are the same.

Figure 4 shows the circumferential hysteresis loops of the Co-rich amorphous wire for

the case in which the azimuthal magnetic field, generated by a current flowing through the wire, is parallel to the direction of the wire magnetization in the outer shell. Since the axial component of the remanent magnetization reduces as a function of the applied tension stress, one should expect the remanent azimuthal magnetization to show an opposite behaviour, as is indeed seen from figure 4.

4. Discussion and conclusions

Due to the absence of magnetocrystalline anisotropy, it is the relatively weak magnetoelastic interactions that determine the magnetization distribution in soft amorphous ferromagnetic wires. The distributions are related to the residual quenching stresses as well as to the externally applied ones. To investigate the effect of the different types of stress on the wire magnetization, here we present a simple model which allows a strict theoretical consideration. The crucial point of the theory is the radial dependence of the diagonal components of the residual stress tensor of the amorphous wire. In principle, this is a problem to be solved separately. The recent attempts at calculations [8, 9] of the residual stress tensor components seem to be oversimplified since they are based on the assumption that the residual stresses at any given point within an amorphous wire coincide with the internal stresses produced at the same point by the thermal gradient at the moment of solidification. It should be stressed that this assumption is only a hypothesis which needs to be justified. Instead of considering the thermal gradient stresses as being frozen, one needs to study the time-dependent evolution of these stresses during the cooling process of an amorphous wire up to room temperature. It is necessary to maintain at all times the mechanical equilibrium between the internal core of the wire, which is still liquid, and the outer solidified shell. Also, it is important to take into account the difference between the specific densities of liquid and amorphous alloys. Having obtained the tensor stress components of the amorphous wire as functions of time, $\sigma_{ii}(x,t)$, one can derive the residual stresses asymptotically by means of the relation $\sigma_{ii}^{(q)}(x) \approx \sigma_{ii}(x,t)|_{t\to\infty}$. The present authors intend to carry out these calculations in a separate paper. Nevertheless, it is interesting to ascertain what kinds of the dependencies $\sigma_{ii}^{(q)}(x)$ are able to describe the experimental behaviour of the amorphous wires with negative magnetostriction properly. Note that we cannot use the results of calculations [9, 3] since they predict that the $\sigma_{\rho\rho}^{(q)}$-component is the smallest component near the centre of an amorphous wire. Thus, in accordance with equation (1), the easy anisotropy axis must be radially directed in the inner core region of the amorphous wire. This result seems to exclude the possibility of the existence of a uniformly magnetized core near the centre of Co-rich amorphous wire. In this paper we point out that the situation shown in figure 1(b) is the simplest possible one which leads to the conventional core–shell structure of Co-rich amorphous wire. Of course, some uncertainty in choosing of the radial dependencies of the stress tensor components still remains. Nevertheless, in case of wire with negative magnetostriction, equation (8) is valid for any of the functions $\sigma_{ii}^{(q)}(x)$ until the situation becomes like that shown in figure 1(a) or figure 1(b). Thus, the possibility exists of fitting the experimental data for the different wires correctly.

In general, the predictions of the model considered here are in agreement with the basic magnetic properties of the Co-rich amorphous wire. For example, the experiments described in [13, 16] show that the remanent wire magnetization is a decreasing function of the applied tensile stress. Also, the application of the tensile stress has only little effect on the wire coercive field [16]. The same behaviour can be seen in figure 3(a). Next, the increase of

the remanent magnetization due to the application of the torsional stress (see figure 3(b)) is in agreement with the experiment described in [15]. The important parameter of the theory is the amplitude of the residual quenching stress. This value for the Co-rich amorphous wire is assumed to be of the order of $\sigma_0 \approx 330$ MPa [6]. Then, the absolute values of the applied tensile stresses corresponding to the curves 2 and 3 in figure 3(a) are 33 MPa and 66 MPa, respectively. These are rather low values as compared with the typical value 100–200 MPa of the applied tensile stress used in the experiments described in [13, 16]. This can probably be explained by assuming that the amplitude of the residual quenching stress in Co-rich wire is somewhat larger than that given in [6]. Another possibility is that the saturation magnetostriction constant is a decreasing function of the stress amplitude [22].

In conclusion, a simple theoretical model which takes into account the distribution of the residual quenching stresses throughout the wire volume is shown to describe qualitatively the basic magnetic properties of Co-rich amorphous wire with negative magnetostriction. Nevertheless, more detailed comparison with the experimental data is needed to refine the model and to achieve a deeper understanding of the magnetization processes in the amorphous wires.

Appendix

Here we describe briefly the numerical procedure used in this paper to obtain the radial profile of the magnetization in an amorphous wire at different values of the applied stress. Taking the variational derivatives of the total free energy (7) with respect to the components of the unit magnetization vector one can obtain the reduced components of the effective magnetic field as

$$h_\varphi = \frac{1}{x}\,\frac{\mathrm{d}}{\mathrm{d}x}\left(x\,\frac{\mathrm{d}\alpha_\varphi}{\mathrm{d}x}\right) - \frac{\alpha_\varphi}{x^2} + p\left[\frac{\sigma^{(q)}_{\varphi\varphi}}{\sigma_0}\alpha_\varphi + \frac{\sigma^{(a)}_{\varphi z}}{\sigma_0}\alpha_z\right] \tag{A1}$$

$$h_z = \frac{1}{x}\,\frac{\mathrm{d}}{\mathrm{d}x}\left(x\,\frac{\mathrm{d}\alpha_\varphi}{\mathrm{d}x}\right) - p\left[\frac{\sigma^{(q)}_{zz} + \sigma^{(a)}_{zz}}{\sigma_0}\alpha_z + \frac{\sigma^{(a)}_{\varphi z}}{\sigma_0}\alpha_\varphi\right] + h_0. \tag{A2}$$

Then it is easy to see that the stationary LLG equation which is equivalent to the ordinary differential equation (8) may be written as

$$A(x) = \alpha_z(x)h_\varphi(x) - \alpha_\varphi(x)h_z(x) \equiv 0. \tag{A3}$$

To integrate (A3) numerically for certain given parameters p and h_0 we carry out a numerical procedure which imitates the evolution of some initial magnetization distribution in accordance with the LLG-type equation. We subdivide the cylindrical wire into a great number ($N \approx 10^2$) of thin hollow cylinders with the same axis, supposing that in the range of the ith cylinder, $(i-1)/N \leqslant x \leqslant i/N$, the unit magnetization vector remains constant, $\boldsymbol{\alpha}_i = (0, \alpha_{\varphi,i}, \alpha_{z,i})$. Suppose that at the sth step of the iteration procedure the magnetization distribution has been obtained for all cylindrical layers, $i = 1, 2, \ldots, N$. Then, at the $(s+1)$th step of this procedure the magnetization distribution in the ith cylindrical layer can be calculated by means of the relations

$$\begin{aligned}
\alpha^{(s+1)}_{\varphi,i} &= \alpha^{(s)}_{\varphi,i} + \tau A^{(s)}_i \frac{\kappa\alpha^{(s)}_{z,i} + \tau h^{(s)}_{z,i}}{1 + \tau^2[(h^{(s)}_{\varphi,i})^2 + (h^{(s)}_{z,i})^2]} \\
\alpha^{(s+1)}_{z,i} &= \alpha^{(s)}_{z,i} - \tau A^{(s)}_i \frac{\kappa\alpha^{(s)}_{\varphi,i} + \tau h^{(s)}_{\varphi,i}}{1 + \tau^2[(h^{(s)}_{\varphi,i})^2 + (h^{(s)}_{z,i})^2]}
\end{aligned} \tag{A4}$$

where

$$A_i^{(s)} = \alpha_{z,i}^{(s)} h_{\varphi,i}^{(s)} - \alpha_{\varphi,i}^{(s)} h_{z,i}^{(s)}. \tag{A5}$$

Here τ is the step of the effective 'time' and κ is the damping parameter of the iteration process. Additionally, after every step of the iteration procedure the unit magnetization vector is normalized as

$$\left[\alpha_{\varphi,i}^{(s)}\right]^2 + \left[\alpha_{z,i}^{(s)}\right]^2 = 1 \qquad i = 1, 2, \ldots, N. \tag{A6}$$

Suppose that the iteration process converges for some appropriately chosen parameters τ and κ. Then, in the limit $s \to \infty$ for any cylindrical layer we have the relations

$$\left|\alpha_{\varphi,i}^{(s+1)} - \alpha_{\varphi,i}^{(s)}\right| \to 0 \qquad \left|\alpha_{z,i}^{(s+1)} - \alpha_{z,i}^{(s)}\right| \to 0.$$

Thus, in the limit $s \to \infty$ in accordance with equations (A4) the values $A_i^{(s)}$ uniformly converge to zero for all layers $i = 1, 2, \ldots, N$. From equation (A5) this implies that the discrete analogue of equation (A3) is obeyed for the magnetization distribution obtained as a result of the iteration procedure. Note that for the convergence of the iteration process a smooth enough initial magnetization distribution must be chosen on the basis of physical considerations. For example, calculating the magnetization distribution in the wire for various values of external magnetic field one may choose a stable magnetization configuration, obtained previously for some value of h_0, as the initial one in order to calculate the corresponding magnetization configuration for a slightly larger or smaller value of h_0. As the criterion for the termination of the iteration process, we use the condition $\Delta\psi_{\max} \leqslant 10^{-4}$ [12, 21], where $\Delta\psi_{\max}$ is the maximal angle of the unit magnetization vector with the normalized effective field vector in the same numerical cell. Typical values of iteration parameters were $\tau = 10^{-5}$ and $\kappa = 0.2$.

References

[1] Squire P T, Atkinson D, Gibbs M R J and Atalay S 1994 *J. Magn. Magn. Mater.* **132** 10
[2] Vazquez M and Chen D-X 1995 *IEEE Trans. Magn.* **31** 1229
[3] Vazquez M and Hernando A 1996 *J. Phys. D: Appl. Phys.* **29** 939
[4] Mohri K, Kohzawa T, Kawashima K, Yoshida H and Panina L V 1992 *IEEE Trans. Magn.* **28** 3150
[5] Beach R S and Berkowitz A E 1994 *Appl. Phys. Lett.* **64** 3653
[6] Mohri K, Humphrey F B, Kawashima K, Kimura K and Mizutani M 1990 *IEEE Trans. Magn.* **26** 1789
[7] Vonsovski S V 1971 *Magnetism* (Moscow: Nauka) (in Russian)
[8] Lui J, Malmhall R, Arnberg L and Savage S J 1990 *J. Appl. Phys.* **67** 4238
[9] Velazquez J, Vazquez M, Hernando A, Savage H T and Wun-Fogle M 1991 *J. Appl. Phys.* **70** 6525
[10] Takajo M, Yamasaki J and Humphrey F B 1993 *IEEE Trans. Magn.* **29** 3484
[11] Isomura R 1961 *J. Japan Inst. Met.* **47** 936
[12] Usov N A and Peschany S E 1993 *J. Magn. Magn. Mater.* **118** L290
[13] Aragoneses P, Blanco J M, Gonzalez J and Vazquez M 1993 *IEEE Trans. Magn.* **29** 3475
[14] Antonov A, Dykhne A, Lagar'kov A and Usov N 1997 *Physica* A **241** 425
[15] Gomez-Polo C, Reininger T, Vazquez M and Kronmuller H 1993 *IEEE Trans. Magn.* **29** 3481
[16] Knobel M, Sanchez M L, Velazquez J and Vazquez M 1995 *J. Phys.: Condens. Matter* **7** L115
[17] Landau L D and Lifshitz E M 1987 *Theory of Elasticity* (Moscow: Nauka) (in Russian)
[18] Rao K V, Humprey F B and Costa-Kramer J L 1994 *J. Appl. Phys.* **76** 6204
[19] Chen D-X, Gomez-Polo C and Vazquez M 1993 *J. Magn. Magn. Mater.* **124** 262
[20] Schabes M E 1991 *J. Magn. Magn. Mater.* **95** 249
[21] Usov N A and Peschany S E 1994 *J. Magn. Magn. Mater.* **135** 111
[22] Hernando A, Gomez-Polo C, Pulido E, Rivero G, Vazquez M, Garcia-Escorial A and Barandiaran J M 1990 *Phys. Rev.* **42** 6471